11th International Conference
1-3 July 2013
Pisa
RASD 2013

RECENT ENHANCEMENTS TO THE NASA LANGLEY STRUCTURAL ACOUSTICS LOADS AND TRANSMISSION (SALT) FACILITY

Stephen A. Rizzi, Randolph H. Cabell and Albert R. Allen

NASA Langley Research Center
Structural Acoustics Branch
Hampton, Virginia 23681 USA
Email: stephen.a.rizzi@nasa.gov, randolph.h.cabell@nasa.gov, albert.r.allen@nasa.gov

Keywords: Reverberant room, transmission loss, absorption

ABSTRACT

The Structural Acoustics Loads and Transmission (SALT) facility at the NASA Langley Research Center is comprised of an anechoic room and a reverberant room, and may act as a transmission loss suite when test articles are mounted in a window connecting the two rooms. In the latter configuration, the reverberant room acts as the noise source side and the anechoic room as the receiver side. The noise generation system used for qualification testing in the reverberant room was previously shown to achieve a maximum overall sound pressure level of 141 dB. This is considered to be marginally adequate for generating sound pressure levels typically required for launch vehicle payload qualification testing. Recent enhancements to the noise generation system increased the maximum overall sound pressure level to 154 dB, through the use of two airstream modulators coupled to 35 Hz and 160 Hz horns. This paper documents the acoustic performance of the enhanced noise generation system for a variety of relevant test spectra. Additionally, it demonstrates the capability of the SALT facility to conduct transmission loss and absorption testing in accordance with ASTM and ISO standards, respectively. A few examples of test capabilities are shown and include transmission loss testing of simple unstiffened and built up structures and measurement of the diffuse field absorption coefficient of a fibrous acoustic blanket.

1. INTRODUCTION

Research into the design and optimization of the acoustic properties of aerospace structures often requires testing to quantify a structure's response to an acoustic field, or to quantify the acoustic absorption of a structure or material. Acoustic testing may also be required in order to qualify structures or components that will be exposed to high acoustic fields in service. The Structural Acoustics Loads and Transmission (SALT) facility at the NASA Langley Research Center is used to conduct these types of tests to support NASA programs and external customers. The SALT facility consists of an anechoic room, reverberant room, and window connecting the two rooms. The facility can be configured to conduct different standard acoustical tests, such as transmission loss, acoustic absorption, and hardware qualification. Past usage of the facility has included measurements of the vibroacoustic characteristics of aerospace components such as aircraft sidewalls [1, 2], noise treatment concepts [3, 4], and for qualification testing [5].

Although the characteristics of the facility have been discussed previously [6], recent modifications have enhanced the facility's capability to generate very high sound levels. These enhancements consist of two acoustic horns driven by airstream modulators, associated air handling and amplifiers to drive the modulators, and controller software to produce a desired spectral shape at the high sound levels. In addition, a planar traversing intensity probe array was installed in order to automate the process for measuring transmission loss of structures. A new adaptor frame has also been constructed to hold transmission loss test articles and minimize facility interactions at panel boundaries.

This paper discusses the characteristics of the SALT facility with the addition of these recent enhancements. This includes characteristics of the anechoic and reverberant rooms for absorption and transmission loss testing, and the high sound level generation capability in the reverberant source room.

2. FACILITY DESCRIPTION

A schematic of the SALT facility is shown in Figure 1. The 278 m^3 reverberant room, shown on the right side of the figure, is structurally isolated from the rest of the building and measures approximately 4.5 m x 6.5 m x 9.5 m (h x w x l). The room walls and ceiling are splayed to diminish the effects of standing waves between opposite surfaces and are separated by a 0.25 m air gap from the surrounding 0.46 m thick concrete building walls. The total surface area of the walls, floor and ceiling is approximately 290 m^2. A photograph of the reverberant room is shown in Figure 2 in a high-intensity reverberant test configuration. The anechoic room, on the left side of the figure measures 4.57 m x 7.65 m x 9.63 m (h x w x l), from wedge tip to wedge tip, for a volume of 337 m^3. The double walls of the room consist of concrete and gypsum board and were designed to provide 54 dB of sound attenuation at 125 Hz. More than 4850 open-cell, polyurethane acoustic wedges cover the walls, ceiling, doors, and floor in the anechoic room. A movable partition covered with acoustic wedges can be placed in front of the transmission loss (TL) window when needed, and wedges can be removed from the floor to create a hemi-anechoic configuration.

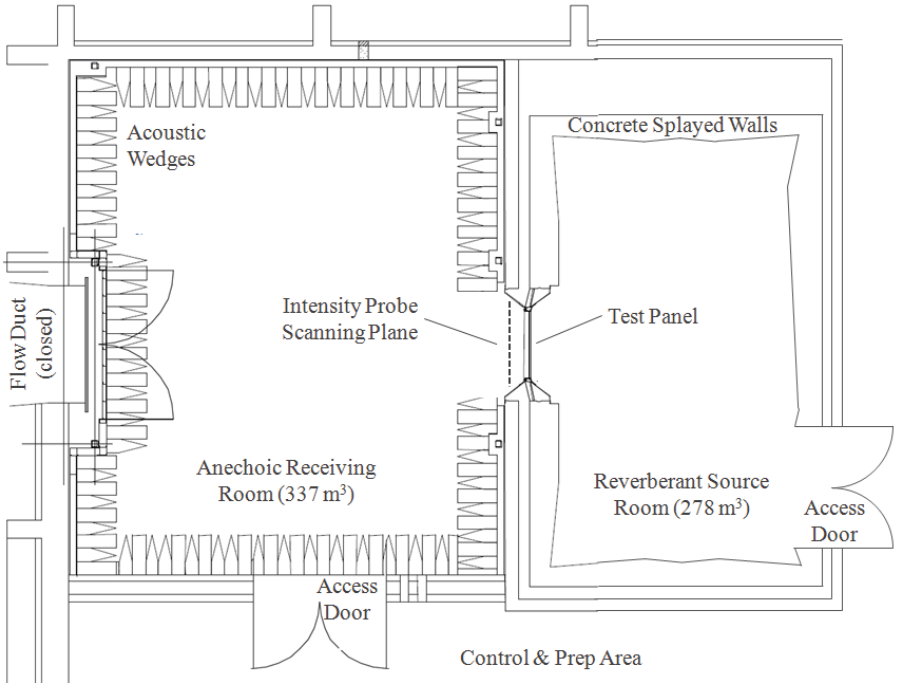

Figure 1: NASA Langley SALT facility showing reverberant and anechoic rooms configured for transmission-loss testing.

Figure 2: Photograph of SALT reverberant room shown configured for high-intensity acoustic testing with airstream modulators coupled to 35 Hz (large) and 160 Hz (small) horns.

The TL window can accommodate test structures up to 1.41 m x 1.41 m, although smaller test structures can be accommodated using an adaptor frame. For most testing, a general purpose adaptor frame is used that reduces the window opening down to 1.19 m x 1.19 m. The frame, shown in Figure 3, consists of a 152 mm wide sandwich of medium density fiberboard (MDF) bonded between two 6.4 mm thick aluminum face sheets. This adaptor was designed to reduce facility modal interactions at lower frequencies [7], although this is often unavoidable when dealing with stiff test structures. Clamping bars are typically used to at the interface between the adaptor and the test article to improve the uniformity of the clamping force.

Figure 3: Aluminum/MDF sandwich adaptor frame (left) with a cross-section view (right).

When needed, such as during absorption and qualification testing in the reverberant room, the TL window can be closed off with a rigid blank made from MDF. During high-intensity qualification testing in the reverberant room, the MDF blank is mounted with an offset from

the window, which provides a vent path for air used by the airstream modulators. The offset panel, painted with the NASA logo, can be seen in the middle of Figure 2.

2.1 Data Acquisition and Control

A schematic of the SALT data acquisition and control systems is shown in Figure 4. Most data and control signals are routed through a Precision Filter 464k 128 input x 128 output programmable patch. Using the switch, input and output signals can be easily routed to acquisition and control hardware depending on the test configuration, without physical rewiring.

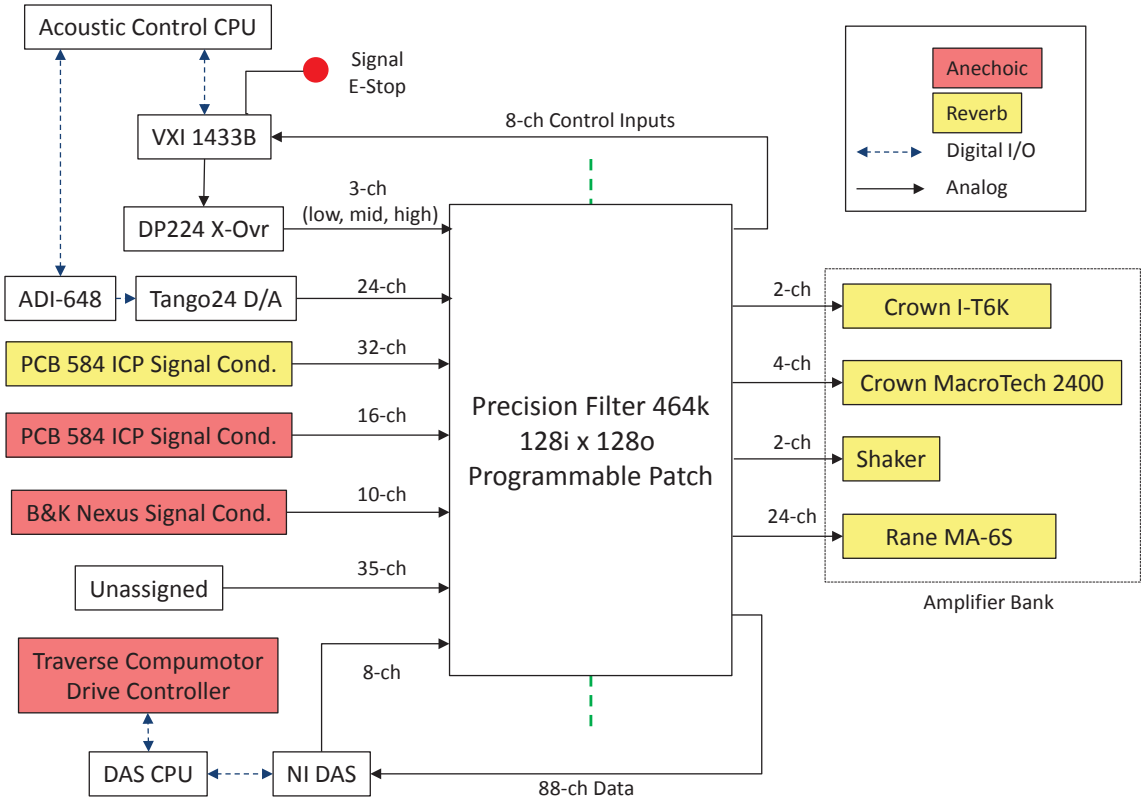

Figure 4: Schematic of SALT data acquisition and control systems.

A data acquisition system (DAS) computer, located at the lower left of the schematic, hosts various data acquisition software including National Instruments (NI) LabView, MATLAB, and M+P International Smart Office Analyzer. The DAS computer is connected to a seventeen-slot PXI chassis that can accommodate any combination of A/D or D/A cards, as needed for a particular test. For most testing, the chassis is populated with eleven 24-bit/8-channel NI 4472B A/D cards for acquiring responses of individual microphones, intensity probes, or other instrumentation.

The particular software and hardware used to generate drive signals for noise or vibration sources in the reverberant room depends on the type of test being conducted. For absorption testing, drive signals are generated on the DAS computer by a 16-bit/8-channel NI 6733 D/A card in the PXI chassis. For all other testing, drive signals are generated on a second computer, labeled the “Acoustic Control CPU” in the schematic, in either an open- or closed-loop configuration. The open-loop configuration is used for transmission loss testing. In this configuration, the digital audio workstation software Audition is used to play up to twenty-four pre-generated signals simultaneously via a 24-bit/64-channel RME ADI-648 digital audio interface with three, 8-channel Frontier Tango-24 D/A converters. This software and

hardware combination provides the capability to drive each speaker in the reverberant room independently of all other speakers with a signal of arbitrary spectral shape. Individual gains in the Audition software are adjusted to obtain a desired overall sound pressure level in the reverberant room.

The closed-loop configuration is used to produce a specified 1/3-octave band reverberant acoustic excitation for high-intensity room acoustic tests. Closed-loop refers to the fact that the sound spectrum in the reverberant room is monitored and used to determine appropriate drive signals to obtain the desired spectrum. In this capacity, the Acoustic Control CPU runs M+P International Acoustic Control software, which generates its drive signal via a VTI Instruments VXI 1433B front-end incorporating up to eight control inputs. Because the controller is typically used to generate a high-intensity acoustic environment for qualification testing, a hardware emergency stop button may be used to terminate the drive signal. Depending on the application, the drive signal may be sent to a XTA Electronics DP224 hardware crossover, with up to three of its four outputs sent via the patch to one or more amplifiers. The acoustic control system is discussed more fully in Section 2.3.2.

In all test configurations, the drive signals are sent through the programmable patch for routing to amplifiers, whose outputs are directed to the sources in the reverberant room.

2.2 Instrumentation

The acoustic excitation in the reverberant room is measured using pre-polarized microphones with an appropriate preamplifier. For excitation levels below 135 dB, G.R.A.S type 46AQ 12.7 mm (½ in) random incidence microphones are used. For high-intensity applications, PCB type 377A12 6.35 mm (¼ in) pressure field microphones are used. In both cases, signal conditioning is provided by 16-channel PCB type 584 ICP signal conditioning units, whose outputs are wired to the programmable patch inputs for routing to the DAS and/or acoustic control systems. For transmission loss and absorption testing, twelve microphones are suspended from the ceiling at heights ranging from 1.1 to 2.7 m off the floor, and at a variety of locations around the room. This arrangement is used to estimate the mean and variance of the sound pressure level in the room. For closed-loop qualification testing, up to eight microphones are used. These are typically arranged at various heights in a circular configuration about the test article.

For transmission loss testing, the acoustic response transmitted through a test article into the anechoic room is measured using 12.7 mm (½ in) B&K 3599 intensity probes, with signal conditioning provided by B&K Nexus conditioning amplifiers. To accelerate testing, five intensity probes are evenly space along a thin, vertical pole on the anechoic side of the TL window, as shown in Figure 5. The pole is traversed horizontally and vertically using stepper motors under the command of a Compumotor drive controller. Motion of the traverse is directed by a MATLAB-based data acquisition system running on the DAS computer, as shown in Figure 4. This approach provides an efficient and automatic implementation of the discrete point method for intensity measurement, as described in ASTM 2249 [8]. A scan grid is defined for each test article based on considerations of test duration, frequency range, and complexity of the intensity field. The offset distance between the intensity measurement plane and the test article can be adjusted from approximately 0.127 m to 0.381 m to accommodate test articles with deep stiffeners or highly reactive intensity fields [9]. In all cases the measurement plane extends to the 45° walls surrounding the window aperture to fully enclose the structure's radiation path. A curved array can also be used to measure sound radiation from curved test articles [10].

Figure 5: Vertical array of five intensity probes (left side) used for TL testing. A PRSEUS composite test panel is shown installed in the aluminum/MDF sandwich adapter frame.

For frequencies between 100 Hz and 6.3 kHz intensity probes with a 12 mm spacer between the microphones provide nearly unbiased measurements. This frequency range can be extended to 10 kHz with the application of a high frequency pressure correction [11]. The correction compensates for the underestimation of intensity at high frequencies that is inherent to the use of free-field microphones in intensity probes. The correction is computed from the electrostatic actuator response recorded during the manufacturer's calibration.

Additional instrumentation needed for a particular test, such as IEPE accelerometers for measuring a structure's dynamic response, are readily conditioned and routed to the acquisition system using the programmable switch. Non-contacting structural dynamic response measurements can also be made from either the reverberant or anechoic rooms using a Polytec PSV-300 scanning laser Doppler vibrometer, which utilizes a separate DAS not shown in Figure 4.

2.3 Acoustic Sources

The SALT facility is equipped with a variety of sources for generating acoustic excitation in the reverberant room. Those used in TL, absorption and qualification testing are next discussed.

2.3.1 TL and Absorption Testing

For TL and absorption testing where sound levels in the reverberant room rarely need to exceed 130 dB, a combination of high-frequency compression drivers and low to mid-frequency loudspeakers are used. The compression drivers consist of fifteen BMS model 4590 co-axial drivers, each with a passive 6.5 kHz crossover, and three JBL 2446H drivers. Fifteen of these drivers are installed on the two walls adjacent to the wall containing the TL window; the other three are mounted on the wall opposite the TL window. Six JBL JRX115i two-way loudspeakers are used to provide low to mid-frequency excitation (<1 kHz) in the reverberant room. Four are ceiling mounted in the corners of the room and two are floor standing in opposite corners of the room. Power to the compression drivers and loudspeakers is provided by a bank of Rane MA-6S amplifiers, see Figure 4.

2.3.2 Qualification Testing

For qualification testing, the performance of a noise generation system comprised of two Cerwin-Vega VIS-218 subwoofers, two Ling EPT94B pneumatic drivers, and six compression drivers was previously characterized [12]. The system was found to be capable of producing desired test spectra below 141 dB overall sound pressure level (OASPL) over

the 31.5 – 2k Hz 1/3-octave band range [12]. This system has the attractive feature of generating moderately high levels with a relatively low noise floor of 107 dB. Greater levels however are required to simulate external loads associated with current and future launch vehicles.

To better address these requirements, an effort was initiated in 2006 to design and construct an additional high-intensity noise generation system for qualification testing. The system utilizes two Wyle WAS 3000 airstream modulators, one of which is coupled to a folded exponential horn with a cutoff frequency of 35 Hz, and the other coupled to a smaller exponential horn with a cutoff frequency of 160 Hz (see Figure 2). Each airstream modulator is supplied with a continuous 2.04 atm (30 psi) air supply. Air is discharged around a standoff panel in the TL window, through the anechoic room and to the outside via a flow duct. The air-on background noise level associated with this system is 124 dB. The modulators are serviced by a 2-channel Crown I-T6000 amplifier. The eighteen aforementioned compression drivers are used for high-frequency noise generation.

Qualification testing generally has strict requirements on sound exposure time and maximum sound levels, to ensure an adequate test has been conducted without overstressing the component. To satisfy these requirements, a closed-loop control strategy was implemented that controls the sound spectrum in the room. The control strategy takes advantage of the frequency response of each component. Shown in Figure 6 is the frequency response of both horns when individually subjected to an open-loop white noise input. Measurements were acquired using eight 6.35 mm (¼ in) high-intensity microphones arranged in a 3.96 m diameter circle centered in the reverberant room, at heights ranging from 1.12 – 2.51 m off the floor. The compression drivers were previously determined to operate best above 1 kHz. Based on this data, the control strategy shown in Table 1 was ultimately adopted. Note that a second pass of gain staging on the compression drivers was used to achieve a higher gain on the drive signal without clipping the signal.

Table 1: Control strategy used for high-intensity noise generation system.

Source	1/3-Octave Control Range (Hz)	DP224 Crossover settings			
		Path	High Pass Filter*	Low Pass Filter*	Gain (dB)
35 Hz Horn	40 – 400	In A → Out 1 (Low)	24.8 Hz	281 Hz	6
160 Hz Horn	500 – 800	In A → Out 2 (Med)	445 Hz	891 Hz	12
Compression	1000 – 4000	In A → Out 3 (In B)	891 Hz	5.04 kHz	0
		In B → Out 4 (High)	707 Hz	5.24 kHz	12

* 24 dB Linkwitz-Riley

The effectiveness of the controller is demonstrated for the 35 Hz horn (Figure 7), the 160 Hz horn (Figure 8), and for the combined system (Figure 9). The bars represent the control level obtained from the average of the eight control microphones. Note that the control ranges shown in these figures reflect preliminary settings before those indicated in Table 1 were settled upon. In these and subsequent closed-loop control plots, the green line represents the 1/3-octave band set point, the yellow lines represent a user-selected ±3 dB deviation from the set point, and the red line represents a user-selected +6 dB abort limit. As configured, up to five bands may exceed the abort limit. A ±3 dB alarm limit and +6 dB abort limit was also specified on the OASPL. The results for the combined system demonstrate an overall control range of 40 Hz to 4 kHz for an OASPL of 137 dB. The limiting factor for a flat response is the performance of the compression drivers. However, this is not a significant factor for most shaped qualification test spectra, as will be shown in Section 4.1.

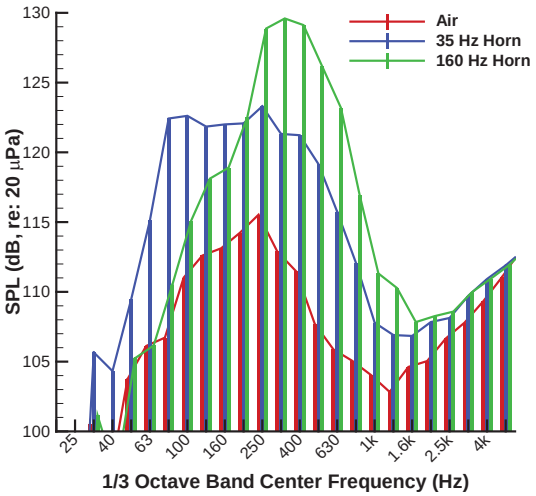

Figure 6: Frequency response of WAS3000 coupled to 35 and 160 Hz horns.

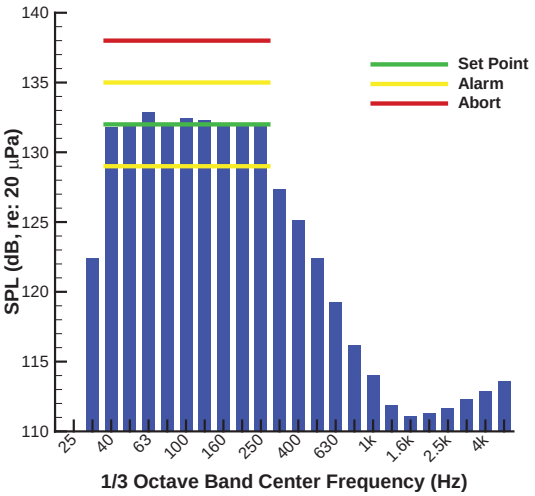

Figure 7: Control of WAS3000 coupled to 35 Hz horn (40-250 Hz).

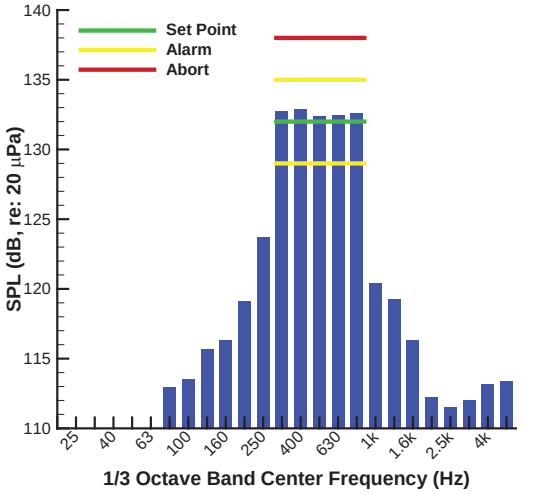

Figure 8: Control of WAS3000 coupled to 160 Hz horn (315-800 Hz).

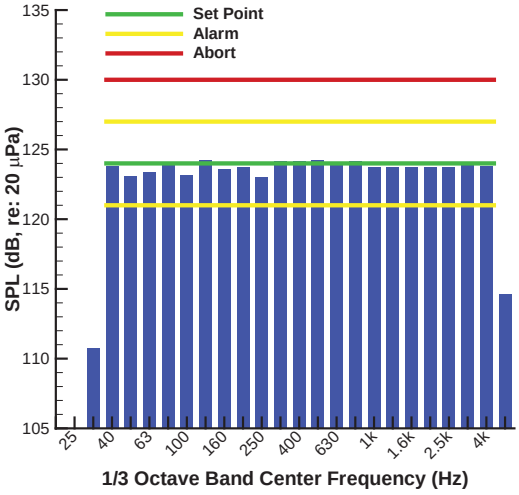

Figure 9: Control of combined high-intensity noise system (40-4k Hz).

3. FACILITY CHARACTERIZATION

This section describes different measurements that are used to quantify the acceptable operating frequency range of the reverberant source room and anechoic room. As most testing in the facility concerns broadband noise sources, the frequency ranges are given here in terms of 1/3-octave band center frequencies.

3.1 Reverberant Room

Several criteria are given in different standards for determining the adequacy of a room for creating a reverberant sound field. For example, the ISO 354 standard, used to determine sound absorption of materials, specifies a maximum allowable room absorption area, denoted here as $A_{max,}$ as a function of 1/3- octave center frequency. On the other hand, the ASTM E90 standard, which is referenced by the ASTM E2249 standard for TL measurement using the intensity technique, gives A_{max} as $V^{2/3}/3$, where V is the room volume. This corresponds to A_{max} = 14.2 m^2 for the reverberant room in SALT. The E90 standard acknowledges that meeting this absorption area requirement may not be feasible at frequencies above 2 kHz. It

further states that absorption may be increased below the Schroder frequency, $f = 2000/V^{1/3}$, to comply with other standards, but not more than three times A_{max}. Yet another criterion can be found in ISO 3741, the standard for determining sound power and sound energy levels in reverberant rooms. This standard requires that the average sound absorption coefficient $\bar{\alpha} = A/S$ be less than $\bar{\alpha}_{max} = 0.16$ below the Schröder frequency, and be less than $\bar{\alpha}_{max} = 0.06$ above the Schröder frequency. Here A is the absorption area of the room and S is the room surface area.

Table 2 provides an overview of recently measured reverberant room characteristics by 1/3-octave center frequency, in relation to the previously mentioned criteria. For these measurements, the room was completely empty, except for the 18 high-frequency, wall-mounted compression drivers. The acoustic horns and all but one low-frequency loudspeaker were removed from the room during testing. The low-frequency loudspeaker acted as the source. In addition, a heavy panel was installed in the TL window to minimize energy losses to the anechoic room.

Table 2: Empty reverberant room characteristics from [13] compared with a selection of standard criteria.

One-third Octave Band Center Frequency	Mean Reverberation Time	Equivalent Sound Absorption Area	ISO 354	ASTM E90	Absorption Coefficient	ISO 3741
[Hz]	T_{20} [s]	$A(T_{20})$ [m^2]	A_{max} [m^2]	A_{max} [m^2]	$\bar{\alpha}$(T20)	$\bar{\alpha}_{max}$
80	14.81	2.99		42.7	0.01	0.16
100	12.81	3.44	8.1	42.7	0.01	0.16
125	13.14	3.33	8.1	42.7	0.01	0.16
160	13.61	3.16	8.1	42.7	0.01	0.16
200	12.41	3.41	8.1	42.7	0.01	0.16
250	10.95	3.8	8.1	42.7	0.01	0.16
315	10.44	3.87	8.1	42.7	0.01	0.16
400	9.79	3.97	8.1	14.2	0.01	0.06
500	8.13	4.69	8.1	14.2	0.02	0.06
630	7.65	4.8	8.1	14.2	0.02	0.06
800	6.7	5.38	8.1	14.2	0.02	0.06
1000	6.19	5.67	8.7	14.2	0.02	0.06
1250	5.79	5.89	9.4	14.2	0.02	0.06
1600	5.1	6.57	10	14.2	0.02	0.06
2000	4.55	7.19	11.9	14.2	0.03	0.06
2500	3.78	8.55	13.1		0.03	0.06
3150	3.45	8.71	15		0.03	0.06
4000	2.86	9.76	16.2		0.04	0.06
5000	2.12	12.86	17.5		0.05	0.06
6300	1.62	15.66			0.06	0.06
8000	1.26	17.25			0.06	0.06

Mean reverberation times, listed in in column two, show the expected decrease with increasing frequency above 160 Hz. Because measurement of the full 60 dB decay time is generally not possible due to signal-to-noise limitations, the T_{20} values are provided, which are the 60 dB reverberation times estimated from the early 20 dB decays. The equivalent sound absorption areas of the room, listed in column three, are below the maximum allowable values from ISO 354 and ASTM E90, listed in columns four and five. Sabine absorption

coefficients, shown in column six, are equal or below the maximum value allowed by ISO 3741 from 80 Hz to 6 kHz. In general, the data indicate the room is able to generate adequately diffuse fields for absorption area and TL measurements according to the standards for those measurements. The reader is referred to [13] for a more comprehensive assessment of the room incorporating various other criteria and different room conditions.

3.2 Anechoic Room

The purpose of the anechoic and hemi-anechoic rooms is to provide a free-field or a partly free-field environment for sound power, sound pressure level, sound intensity and directivity measurements of acoustic sources. Characteristics of the anechoic room, measured in 1999 [6], are only summarized here as the configuration of the room has not changed since those measurements were made.

Characterization of the anechoic room follows the procedure described in ISO 3745, which specifies maximum allowable differences between inverse-square-law calculations and measured levels at varying distances from a sound source in the room. Acoustic measurements were conducted for both an anechoic and hemi-anechoic room, using a 0.241 m diameter Kevlar cone loudspeaker in the corner of the anechoic room and a four-microphone measurement pole placed at various distances from the loudspeaker. The loudspeaker was positioned halfway between the floor and the ceiling with horizontal clearances of 1.30 m and 1.75 m to the nearest acoustic foam wedge tips. An amplified pink noise signal was supplied to the loudspeaker. Deviations from the inverse-square-law sound pressure levels were calculated from 80 Hz to 12.5 kHz and normalized to the sound level measured at a far-field microphone 2.74 m from the source.

In the anechoic configuration, the deviations from inverse-square-law were all within the requirements specified in the standard, except the farthest measurement locations below 250 Hz. At these locations, the measurement microphones were close to the room corner opposite the sound source. The excess deviations were attributed to long wavelength sound reflecting from the corners of the room. In the hemi-anechoic configuration, deviations were within the range permitted by the international standard, except for three corner measurement locations at 80 Hz one corner location at 100 Hz.

Deviations from inverse square law were also measured and calculated when the sound source was hung in front of the TL window. A seven-ply fiberboard insert was placed in the window and covered with 0.914 m thick acoustic foam to minimize acoustic reflections from the insert. Deviations were within the criteria of ISO 37452 except for a few locations near the fiberboard insert and the opposite room wall below 160 Hz. These higher deviations were attributed to long wavelength sound reflecting from the nearby wall and interacting with the incident sound.

These measurements indicate the anechoic room provides an adequate approximation of a free-field acoustic environment from 80 Hz to 12.5 kHz, although care should be taken to keep an adequate separation distance between the microphones and walls of the room below 250 Hz.

4. APPLICATIONS

This section discusses test results that illustrate the capabilities of the SALT facility for qualification, TL and acoustic absorption testing.

4.1 High-Intensity Qualification Testing

The sound generating capability of the new high-intensity system is next demonstrated for three relevant test spectra; a payload launch environment for the X-37 Orbital Test Vehicle [14], a payload acoustic environment for the Orbital Sciences Corporation Minotaur IV [15],

and a typical external acoustic launch environment. All tests were performed in an empty reverberant room, i.e., without a test article installed.

The acoustic spectrum tested for the X-37 launch environment was generated by bounding acoustic spectra derived from the Atlas V and Delta IV launch environments. This spectrum was previously used to perform room-temperature tests of candidate X-37 hot structure control surfaces including C/SiC and C/C flaperon subcomponents, and a C/C ruddervator subcomponent [5]. The spectrum shown in Figure 10 demonstrates the high level of control achievable with this system. In addition, comparable performance is noted at 6 dB above the reference level, indicating significant margin for accelerated testing.

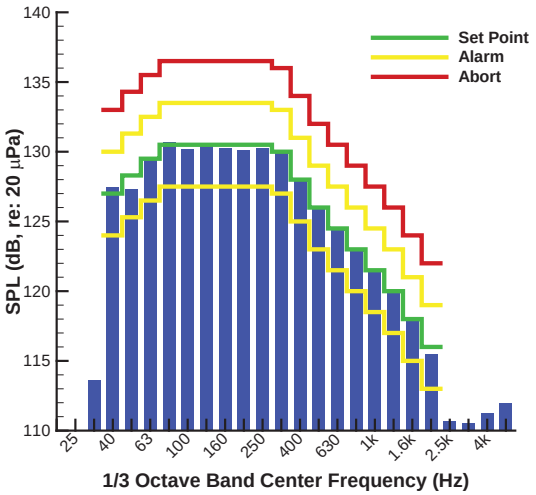

Figure 10: Reference X-37 launch environment (141 dB OASPL).

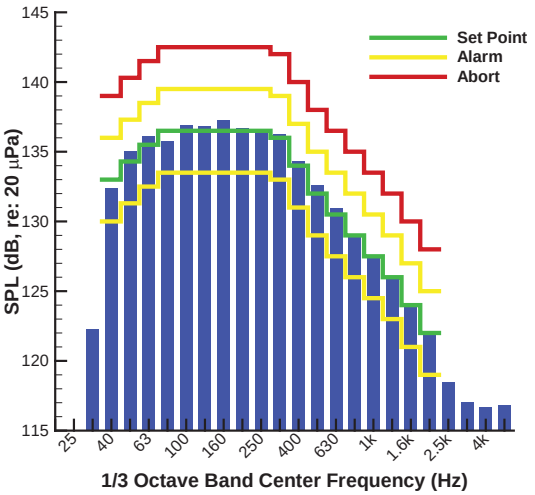

Figure 11: Accelerated X-37 launch environment (+6 dB above reference).

The Minotaur IV payload environment is considered next. This environment has a prominent peak from the 160 to 500 Hz 1/3-octave bands, as seen in Figure 12. Good control is maintained throughout the frequency range. When pushed to the limit, the noise generation system was capable of generating this spectrum 18 dB above the reference level, or 154 dB OASPL, albeit with distortion in the region above 1 kHz. Nevertheless, the spectrum was maintained within the limits specified.

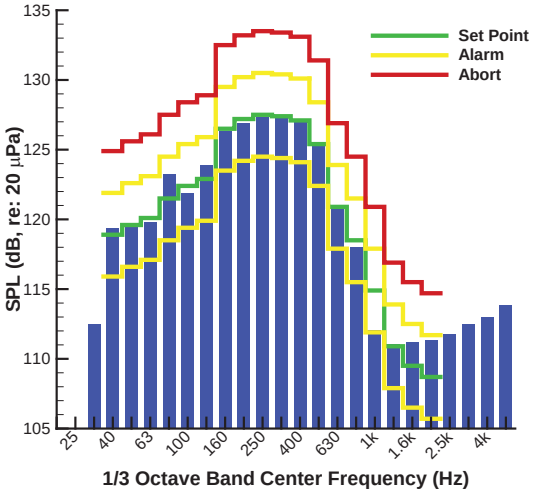

Figure 12: Reference Minotaur IV payload environment (136 dB OASPL).

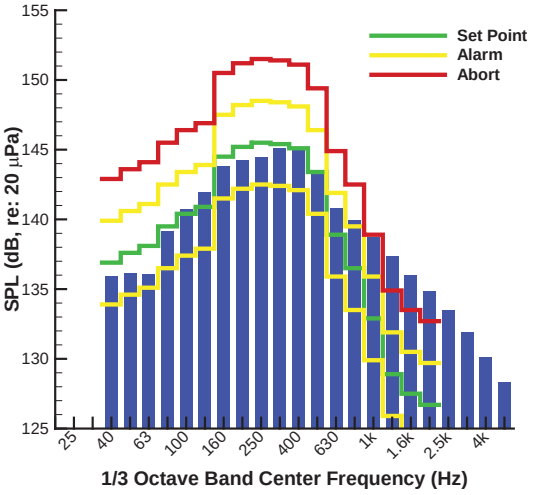

Figure 13: Accelerated Minotaur IV payload environment (+18 dB above ref).

Lastly, a typical external acoustic launch environment is shown in Figure 14. Good control is maintained over the full range. The +3 dB accelerated spectrum shown in Figure 15 is seen to maintain the desired shape.

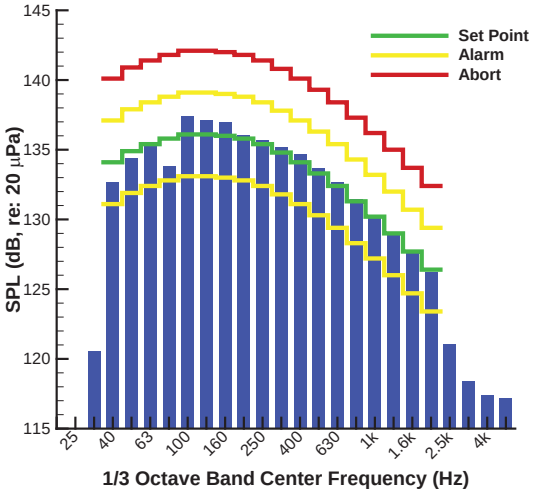

Figure 14: Reference external acoustic environment (147 dB OASPL).

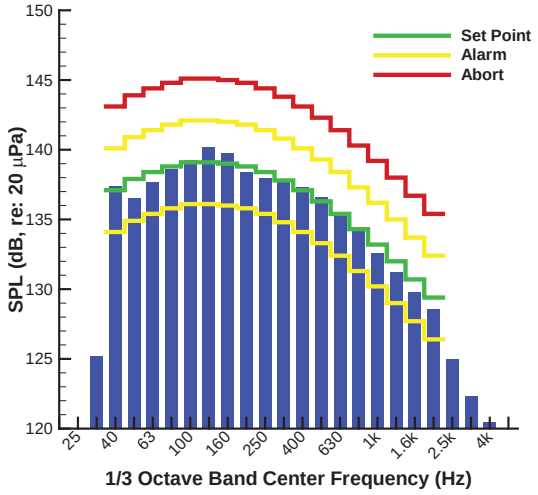

Figure 15: Accelerated external acoustic environment (+3 dB above reference).

The above results demonstrate the ability of the SALT high-intensity noise generation system to perform qualification testing in relevant environments.

4.2 Transmission Loss Testing

4.2.1 Test Method

Measurement of transmission loss is one of the SALT facility's primary functions. These tests are conducted according to the discrete point method described in ASTM E2249 for transmission loss measurement using sound intensity [8]. For TL testing, a test panel is installed in the TL window, drivers in the reverberant source room create a diffuse field, and the array of intensity probes is used to scan the sound power transmitted through the test panel. Each driver in the source room is driven with a signal that is statistically independent from the signal used to drive every other acoustic source. The drive signals are shaped to maintain adequate signal to noise ratio at higher frequencies where TL is typically highest. TL testing is typically conducted in the linear range with space averaged reverberant room levels, L_1, maintained near 100 dB OASPL. The sound level in the room is quantified using the twelve 12.7 mm (½ in) random incidence microphones located randomly throughout the room.

From the ASTM standard [8], the TL is defined as the dB ratio of incident to transmitted power,

$$TL = 10\log_{10}\left(\frac{W_{inc}}{W_{rad}}\right) = \left[L_1 - 6 + 10\log_{10}(S)\right] - \left[\overline{L}_{In} + 10\log_{10}(S_m)\right] \quad (1)$$

where L_1 is the average source room sound pressure level, $\overline{L}_{In}$ is the surface averaged transmitted sound intensity normal to the measurement surface, S is the radiating area of the test article, and S_m is the area of the intensity measurement surface. $\overline{L}_{In}$ is computed from discrete-point intensity measurements made using the array traverse system described previously and shown in Figure 5. Specifically, the measured intensity $\hat{I}_{nk}$ at the k^{th} point is

computed from the imaginary part of the cross spectrum between the microphone pair pressure signals $\hat{p}_1$ and $\hat{p}_1$ using the expression

$$\hat{I}_{nk} = \frac{\mathrm{Im}\left\{\hat{p}_1 \hat{p}_2^*\right\}}{2\rho\omega\Delta r} \tag{2}$$

where ρ is the density of air, ω is the angular frequency, and Δr is the microphone separation distance. The surface averaged sound intensity can then be computed by summing the product of individual $\hat{I}_{nk}$ and their corresponding measurement sub-area, S_{mk}, taking into account the sign of the individual $\hat{I}_{nk}$ in order to account for sound radiating either toward or away from the test article. The surface averaged normal sound intensity level, $\overline{L_{In}}$, is then computed as

$$\overline{L_{In}} = sgn\left(\overline{I_n}\right) 10 \log\left(\frac{\left|\overline{I_n}\right|}{I_0}\right) dB \tag{3}$$

where $\overline{I_n}$ is the surface averaged sound intensity.

The E2249 standard provides two criteria for determination of acceptable measurements when using the discrete point method:

Criterion 1:	$F_2 < L_d$	Adequate Dynamic Range
Criterion 2:	$N > CF_4^2$	Adequate Measurement Array

In Criterion 1, the dynamic capability index of each probe, L_d, is found from $L_d = \delta_{pI_0} - K$, where δ_{pI_0} is the pressure-residual intensity index (PRII) of the probe and K = 10 dB is an error factor. The PRII is measured during field calibration prior to testing. The surface pressure-intensity indicator, F2, is the difference between the pressure level and the unsigned intensity level averaged over the scan area. Adequacy of the measurement array resolution, Criterion 2, depends on N, the number of scan points, and F_4, the field non-uniformity indicator. F_4 quantifies the variation of intensity over the scan plane, and C is a frequency dependent correction factor specified in Table A1.1 in E2249.

4.2.2 Results

TL measurements from a thin unstiffened aluminum panel and a stiffened composite structure are presented here to illustrate the capabilities of the facility. The thin aluminum panel, with dimensions 0.81 mm x 1.22 m x 1.22 m, was installed in the adaptor frame discussed earlier; the ensonified and radiating surface areas of the panel were 1.365 m^2. The scan plane of the intensity probes was offset from the test article by 0.36 m, and the spacing between neighboring scan points was approximately 14 cm. This spacing corresponds to 195 discrete intensity measurement points.

The measured TL of the aluminum panel, with the high frequency correction, is compared with predicted TL in Figure 16. The aluminum panel's TL was predicted using a classical wave approach with a correction for the spatial windowing effects of the finite panel, using the method described in Villot et al. [16] and Vigran [17]. The measurements and predictions show excellent agreement above 125 Hz. At lower frequencies, a number of biasing effects are expected, such as non-diffuseness in the source room, and modal interaction between the test panel and the adaptor frame.

The measurement-acceptability criteria for the aluminum panel data are shown in Figure 17 and Figure 18. In Figure 17, F_2 is well below L_d for all five probe pairs, and thus the dynamic range is adequate. The adequacy of the measurement array is illustrated in Figure 18, where N exceeds CF_4^2 throughout the entire frequency range.

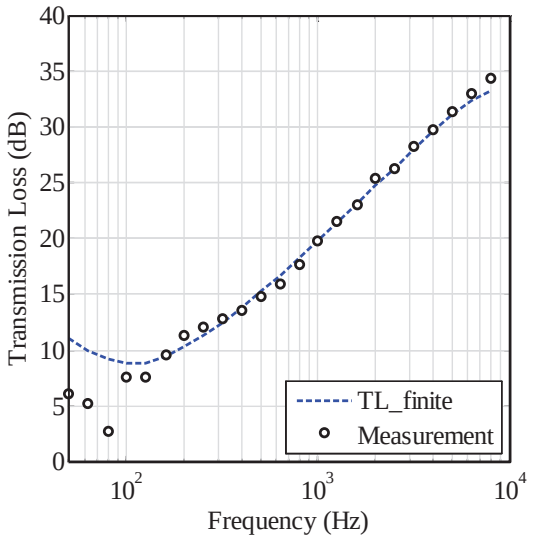

Figure 16: Comparison of TL measurements and prediction for a thin aluminum panel.

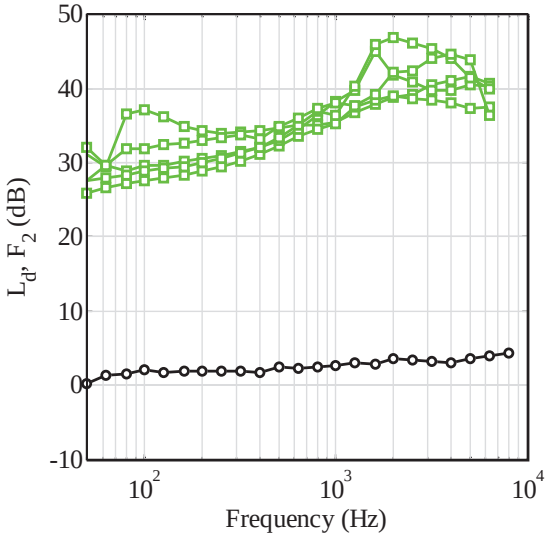

Figure 17: Comparison of *Ld* (-□-) and F_2 (-○-) associated with Figure 16.

The measured TL of a stiffened composite structure, called PRSEUS, is briefly discussed here as a demonstration of typical tests conducted in the facility. PRSEUS (Pultruded Rod Stitched Efficient Unitized Structure) is a fastenerless composite fuselage concept with stitched and co-cured stringer and frame stiffeners, created to explore alternative fuselage architectures able to support loading conditions in unconventional aircraft [18]. The test panel constructed using the PRSEUS method can be seen in the TL window in Figure 5. The TL was measured using the intensity probe array and similar scan settings used on the unstiffened aluminum panel. The measured results are compared with predictions from two finite element based methods of varying computational expense. The first method is a conventional boundary element approach that accounts for the sound radiation from the panel, including scattering and direct radiation from the stiffeners. This method requires considerable computational resources and was only carried out for a portion of the frequency range. A second, more efficient method was also used that ignored scattering and direct radiation from the stiffeners and assumed planar radiation impedance by using a Rayleigh integral approach. The structure, finite element model, and analysis procedures pertaining to this structure can be found in [1].

Measured and predicted TL data for the PRSEUS panel are shown in Figure 19 for a frequency range from 315 to 3150 Hz. The measurements and predictions agree well, although the BEM prediction was only done at four 1/3-octave bands due to the computational expense of that model. The simpler planar-radiator model that ignored effects of the large stiffeners shows good agreement with measured data from 400 Hz to 1600 Hz. Note that comparing predictions and measurements below 315 Hz becomes problematic due to coupling between the stiff PRSEUS panel and the surrounding adaptor frame; this coupling was not represented in the models.

The relatively small deviations between measured and predicted TL for these test panels (<2 dB above 100 Hz for the aluminum panel, and <4 dB from 400 Hz to 3.15 kHz for the PRSEUS panel) provide confidence that the basic data acquisition and post-processing procedures used for computing TL in the SALT facility produce meaningful results.

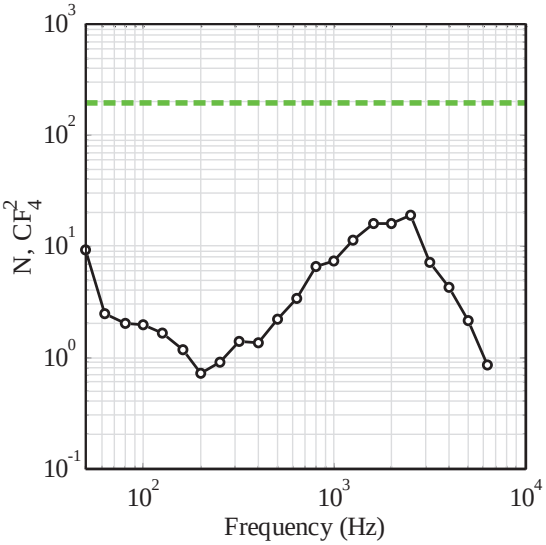

Figure 18: Comparison of N (--) with CF_4^2 (-○-) associated with Figure 16.

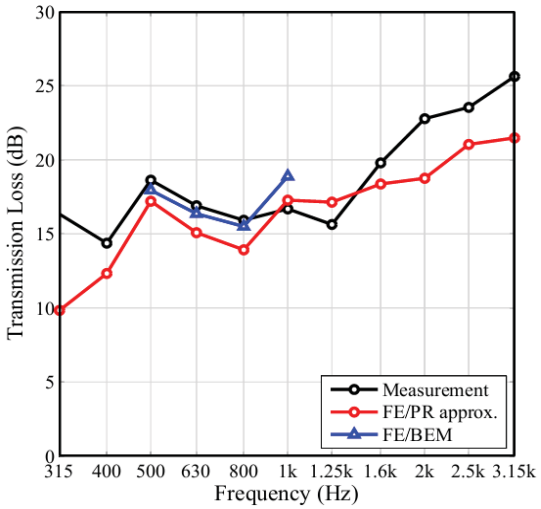

Figure 19: Comparison of TL measurements and predictions for PRSEUS panel.

4.3 Absorption Area Testing

4.3.1 Test Method

The reverberant room can be used to determine the sound absorption of a material following procedures given in ASTM C423-09a and ISO 354:2003(E) [19]. For these tests, a heavy panel is installed in the TL window to minimize energy loss to the anechoic room. Note that with the panel installed, the equivalent sound absorption area in the room is below the maximum allowable equivalent sound absorption area in ISO 354 from 100 Hz to 5 kHz. The absorption measurement procedure is based on measured reverberation times with and without the test specimen in the reverberant room. The resulting reverberation times are then used to compute the equivalent absorption area, A, in a given 1/3-octave band, for the room with and without the test specimen, according to

$$A = 0.9210\frac{Vd}{c} \tag{4}$$

where V is the room volume, c is the speed of sound, and d is the sound decay rate for the octave band. If A_2 denotes the absorption area with the test specimen present in the room and A_1 the absorption area for the empty room, the diffuse field sound absorption coefficient α_d can be determined by

$$\alpha_d = \frac{A_2 - A_1}{S} + \alpha_S\,, \tag{5}$$

where S is the area of the test specimen and α_S is the absorption coefficient attributed to the area covered by the test specimen (assumed to be zero for the hard floor reverberant room). The decay rate attributed to air attenuation is accounted for prior to calculating the absorption area and is a function of the ambient room conditions.

An integrated impulse response method with background noise correction is used to measure the decay curves in the reverberant room [20]. Before each test, the background noise is measured in the room in order to apply it as a correction to the integrated impulse. The test procedure is automated, using the existing loudspeakers and twelve hanging 12.7 mm (½ in) microphones so decay rates can be efficiently measured at multiple combinations of source positions and microphone locations without having to open the doors to the room. The number of source positions can be varied, but for a typical test, the room is excited with five of the wall-mounted compression drivers and three of the low-frequency (ceiling-mounted)

drivers, one driver at a time. The low frequency drivers are used to generate response data from 80 Hz through the 1 kHz 1/3-octave band. For a given 1/3-octave band, the excitation signal sent to a loudspeaker consists of the time-reversed impulse response of the corresponding 1/3-octave band-pass filter. A MATLAB program running on the DAS computer is used to send signals out through the NI 6733 D/A card, and record the microphone responses via the NI 4472B A/D cards.

Decay times are estimated for each speaker-microphone combination and then averaged together. The decay times are computed as $T_{60} = 60/d$, where the decay rate, d, is computed from a log-linear regression of the reverse integrated decay curve for a speaker-microphone combination. The log-linear regression is used to estimate the slope of the decay curve along a 20 dB range starting 5 dB below the peak level [19]. The combination of twelve microphones and 3 low frequency drivers yields 36 decay curves per band; the 5 high frequency drivers yield 60 decay curves per band above 1 kHz. The arithmetic mean of the computed decay times are then calculated (after compensating for air attenuation) and used in equation (4). The variance can also be propagated through the expressions to estimate the uncertainty of A and α_d over the set of unique source and microphone positions.

4.3.2 Results

The absorption measurement procedure was used to measure the diffuse field sound absorption coefficient of a sample of 9.6 kg/m^3, 25.4 mm-thick aircraft grade fiberglass. The sample was cut to cover a 3.66 m x 3.66 m square area and was placed on the floor in a random, centrally located position avoiding close proximity with the room walls. The T_{60} reverberation times measured with and without the sample are shown in Figure 20. As expected, the decay times with the test specimen in the room are less than the decay times without the specimen. The corresponding absorption coefficient is shown in Figure 21. These data also show the expected behavior of α approaching unity at high frequencies. Values of α greater than unity are possible if the edges of the sample absorb a significant amount of sound and those edges aren't included in the absorption area.

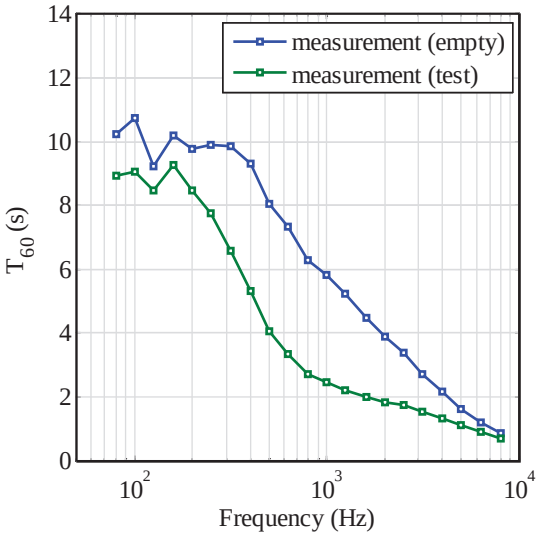

Figure 20: Reverberation time, T60, with and without the fiberglass sample.

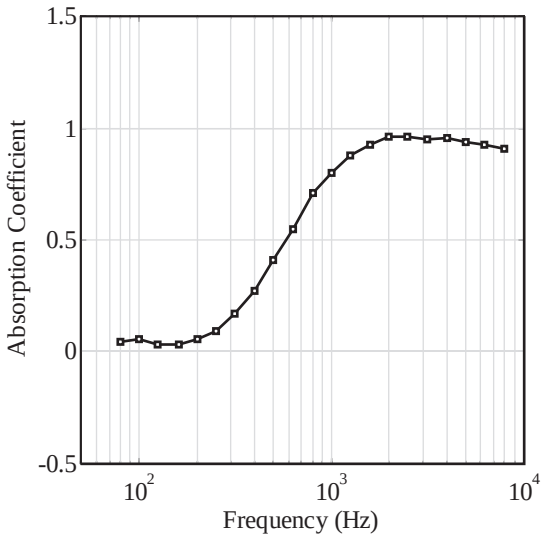

Figure 21: Diffuse field absorption coefficient of the fiberglass.

Determining the overall uncertainty of transmission loss and absorption area measurements acquired using the above procedures requires establishing a budget of uncertainty components and will be the subject of future efforts.

5. CONCLUDING REMARKS

Recent enhancements to the NASA Langley Structural Acoustics and Loads Transmission facility have increased its testing capabilities in a substantial manner. A new high-intensity noise generation system increased the maximum overall sound pressure level to 154 dB, an increase of 13 dB over its prior maximum. The closed-loop control system allowed a uniform spectrum to be maintained over a 40 – 4k Hz bandwidth, and relevant launch spectra to be simulated at and above the specified reference level. The facility is therefore capable of performing high-intensity qualification testing over a range of environments.

Also demonstrated was the ability of the SALT facility to conduct transmission loss and absorption testing. An efficient means of transmission loss testing in accordance with the discrete point method described in ASTM E2249 was demonstrated for a simple unstiffened panel and a stiffened composite structure. A traversing array of intensity probes was employed to reduce test time. Relatively small deviations between measured and predicted TL for these test panels established confidence in the TL measurements made in the SALT facility. Finally, an absorption testing method made in accordance with ASTM and ISO standards was demonstrated using aircraft grade fiberglass. The data showed expected trends in the absorption coefficient as a function of frequency.

The improvements in facility capabilities and demonstration of standard test capabilities position the SALT facility to support future research and development activities within the NASA Aeronautics Research, Exploration Systems, and Science Mission Directorates, as well as external utilization.

ACKNOWLEDGMENTS

This paper is dedicated to the memory of Clyde G. Medley, Jr. (1960-2012), whose support helped enhance the capabilities of the SALT facility. The authors also wish to thank Carlton G. Pike for his role in supporting the high-intensity noise enhancements and in the reported test efforts, and Sajeela Padder (2012 Langley Aerospace Research Student Scholar) for her initial implementation of the sound absorption test method.

DISCLAIMER

The use of trademarks or names of manufacturers in this paper is for accurate reporting and does not constitute an official endorsement, either expressed or implied, of such products or manufacturers by the National Aeronautics and Space Administration.

REFERENCES

[1] Allen, A.R. and Przekop, A., "Vibroacoustic characterization of a new hybrid wing-body fuselage concept," *Proceedings of the Internoise 2012/ASME NCAD meeting*, IN12-321, New York, NY, 2012.

[2] Joshi, P., Mulani, S.B., Slemp, W.C.H., and Kapania, R.K., "Vibro-acoustic optimization of turbulent boundary layer ex-cited panel with curvilinear stiffeners," *AIAA Journal of Aircraft*, Vol. 49, No. 1, pp. 52-65, 2012.

[3] Buehrle, R.D., Gibbs, G., Klos, J., and Mazur, M., "Modeling and validation of damped plexiglas windows for noise control," *44th AIAA/ASME/ASCE/AHS Structures, Structural Dynamics, and Materials Conference*, AIAA-2003-1870, Norfolk, VA, April 7-10, 2003.

[4] Palumbo, D.L. and Klos, J., "Development of quiet honeycomb panels," NASA TM-2009-215954, 2009.

[5] Grosveld, F.W., Rizzi, S.A., and Rice, C.E., "Dynamic response of the X-37 C-C and C-SiC subcomponents exposed to controlled reverberant acoustic excitation," NASA TM-2005-213519, 2005.

[6] Grosveld, F.W., "Calibration of the Structural Acoustics Loads and Transmission Facility at NASA Langley Research Center," *Inter-Noise*, pp. 6, Fort Lauderdale, FL, 1999.
[7] Velicki, A., Yovanof, N.P., Baraja, J., Mathur, G., Thrash, P., and Pickel, R.l., "PRSEUS Acoustic Panel Fabrication," NASA CR-2011-217309, 2011.
[8] ASTM, "Standard test method for laboratory measurement of airborne transmission loss of building partitions and elements using sound intensity," *E2249-02*, 2008.
[9] Jacobsen, F., "Sound intensity measurements," In *Handbook of Noise and Vibration Control*, John Wiley & Sons, pp. 534-548, 2007.
[10] Klos, J., Robinson, J.H., and Buehrle, R.D., "Sound transmission through a curved honeycomb composite panel," *9th AIAA/CEAS Aeroacoustics Conference*, AIAA-2003-3157, Hilton Head, SC, May 12-14, 2003.
[11] Jacobsen, F., Cutanda, V., and Juhl, P., "A numerical and experimental investigation of the performance of sound intensity probes at high frequencies," *Journal of the Acoustical Society of America*, Vol. 103, No. 2, pp. 953-961, 1998.
[12] Grosveld, F.W. and Rizzi, S.A., "Controlled reverberant acoustic excitation capabilities at NASA Langley Research Center," *43rd AIAA Aerospace Sciences Meeting*, AIAA-2005-0421, Reno, NV, January 10-13, 2005.
[13] Grosveld, F.W., "Characterization of the reverberation chamber at the NASA Langley Structural Acoustics Loads and Transmission (SALT) facility," NASA CR-2013-xxxxxx (in preparation), 2013.
[14] "Boeing X-37 (http://en.wikipedia.org/wiki/Boeing_X-37)," Wikipedia, 2013.
[15] "Minotaur IV User's Guide, Release 1.1," Orbital Sciences Corporation 2006.
[16] Villot, M., Guigou, C., and Gagliardini, L., "Predicting the acoustical radiation of finite size multi-layered structures by applyling spatial windowing on infinite structures," *Journal of Sound and Vibration*, Vol. 245, No. 3, pp. 433-455, 2001.
[17] Vigran, T.E., "Predicting the sound reduction index of finite size specimen by a simplified spatial windowing technique," *Journal of Sound and Vibration*, Vol. 325, No. 3, pp. 507-512, 2009.
[18] Sloan, J., "PRSEUS preform for pressurized cabin walls," in *High Performance Composites*, vol. 19, 2011, pp. 50-53.
[19] ISO, "Measurement of sound absorption in a reverberation room," *ISO 354*, 2003.
[20] Chu, W.T., "Comparison of reverberation measurements using Schroeder's impulse method and decay-curve averaging method," *Journal of the Acoustical Society of America*, Vol. 63, No. 5, pp. 1444-1450, 1978.